NATIONAL ADVISORY COMMITTEE FOR AERONAUTICS

TECHNICAL NOTE 1989

SOME EFFECTS OF DENSITY AND MACH NUMBER ON THE FLUTTER SPEED OF TWO UNIFORM WINGS

By George E. Castile and Robert W. Herr

Langley Aeronautical Laboratory
Langley Air Force Base, Va.

Washington
December 1949

NATIONAL ADVISORY COMMITTEE FOR AERONAUTICS

TECHNICAL NOTE 1989

SOME EFFECTS OF DENSITY AND MACH NUMBER ON THE FLUTTER SPEED OF TWO UNIFORM WINGS

By George E. Castile and Robert W. Herr

SUMMARY

Results of sixty-six experimental flutter tests are presented to show some effects of density and Mach number upon flutter speed. Two uniform, cantilever wing models, one having a small amount of sweep, were fluttered through a range of Mach number up to 0.82. The mass ratio, κ, for these models ranged from 0.00375 to 0.11, while Reynolds number varied from 0.266×10^6 to 3.000×10^6. Two testing mediums, having different velocities of sound, were used to obtain flutter at two Mach numbers at the same density.

Multiplying the flutter speeds by a simple compressibility factor superimposed the plots of flutter speeds obtained in the two gases throughout the range of densities, and this correction was indicated to be adequate for the range of parameters considered. An additional correction to the flutter speed was made to account for the change due to the reduced-wave-length parameter. Correcting the experimental flutter speed for both Mach number and wave-length effects resulted in a nearly constant dynamic pressure at flutter. No Reynolds number effect upon flutter speed was indicated except at values below 0.400×10^6. A specific change in tunnel-wall interference had no appreciable effect on the flutter speed.

INTRODUCTION

Present-day trends toward flight at high speeds and high altitudes have led to increasing interest in the flutter speed at low densities and high Mach numbers. An experimental investigation has consequently been made to determine some of the effects of these parameters on flutter speed. These experiments were carried out on two uniform cantilever wings, one unswept and one with 15° sweepback. A study of density effects was made possible by fluttering the models through a wide range of pressure and the Mach number effects were isolated by the use of two testing mediums having different velocities of sound.

In the course of this investigation, correlation of the experimental data required consideration of the effects of the reduced-wavelength parameter and Reynolds number. In addition, the effect of the tunnel wall parallel to the span was studied by changing the distance from wall to model.

SYMBOLS

l	length of model measured along midchord, feet
b	half-chord of model normal to leading edge, feet
a	nondimensional coordinate axis of rotation relative to midchord
r_α	nondimensional radius of gyration relative to axis of rotation
x_α	nondimensional center of gravity relative to axis of rotation
f_α	natural frequency of torsional vibrations, cycles per second
f_h	natural frequency of bending vibrations, cycles per second
f_f	flutter frequency, cycles per second
ρ	density of testing medium, slugs per cubic foot
m	mass of wing per foot of length
M	Mach number
κ	mass ratio $\left(\frac{\pi\rho b^2}{m}\right)$
v	flutter velocity, feet per second
ω	angular flutter frequency, radians per second ($2\pi f_f$)
F	in-phase component of circulation functions (reference 2)
G	out-of-phase component of circulation functions (reference 2)
Λ	sweepback angle of midchord line, degrees

Subscripts:

e	experimental value
1	first mode
2	second mode

APPARATUS

These experiments were performed in the Langley flutter tunnel. The tunnel is of the closed-throat, single-return type in which either Freon-12, air, or a mixture of the two may be used as a testing medium. A characteristic of this tunnel is that Mach number and density of the testing medium can be varied independently. The pressure can be varied from atmospheric to 4 inches of mercury absolute, and a density range from 0.000317 slug per cubic foot in air to 0.0106 slug per cubic foot in Freon-12 is thus provided. The Mach number range of the tunnel is from 0 to approximately 0.92. Flutter was attained at Mach numbers up to 0.82. The mass ratio, κ, for these models ranged from 0.00375 to 0.11. The Reynolds number range was from 0.266×10^6 to 3.000×10^6.

In order to investigate some of the effects of tunnel-wall interference upon flutter speed, two tunnel test sections were employed: one of circular cross section 4.5 feet in diameter; the other, the 4.5 foot section with side walls installed to give a section approximately 2 feet by 4.5 feet as shown in figure 1.

Data were obtained for two different model wings (figs. 2 and 3). The models were built up of solid balsa wood with dural inserts and were mounted rigidly at the top of the test section as cantilever beams at zero angle of attack. Model A had 15° of sweepback whereas model B

had none. Both models incorporated the NACA 16-010 airfoil section. The physical properties of these models were as follows:

Model	A	B
l, feet	2.167	4.0
b, feet	0.167	0.333
m, slugs per foot	0.0099	0.0272
r_α^2, nondimensional	0.107	0.324
a, nondimensional	-0.16	-0.36
x_α, nondimensional	-0.024	-0.238
f_{h_1}, cycles per second	9.4	4.5
f_{h_2}, cycles per second	56	27
f_α, cycles per second	97	47
κ, nondimensional	8.81ρ	12.84ρ

Two sets of strain gages were attached to each model near the root and were connected to a recording oscillograph in order to determine the natural bending and torsional frequencies as well as the flutter frequency.

TEST PROCEDURE

Flutter occurs very suddenly and is usually destructive unless great care is exercised. Since this series of experiments required the physical properties of the models to remain unchanged, preservation of the models was an important consideration. The airspeed in the tunnel was, therefore, brought up gradually until flutter was observed. The airspeed was then reduced immediately in order to prevent destruction of the model. At the point of flutter, an oscillograph record was taken and the tunnel pressure, dynamic pressure, and tunnel temperature were recorded. The percentage of Freon-12 in the testing medium was obtained after each test. The natural bending and torsional frequencies of the model were recorded on the oscillograph after each test in order to ascertain whether the model had been damaged or weakened by flutter. These frequencies did not change a measurable amount throughout the series of tests.

DISCUSSION OF RESULTS

Results of sixty-six experimental flutter tests are presented in tables I and II. As stated in the introduction, effects of density, Mach number, wave length, Reynolds number, and tunnel-wall interference

were partly isolated and the effects of these parameters are shown in figures 4 to 11 and briefly discussed in the following paragraphs. Although density is the principal parameter, corrections for Mach number and wave length must be applied to the flutter speeds before a comprehensive picture of the variation of flutter speed with density can be gained.

Mach number.- Many investigators have studied, theoretically, means of correcting the air forces acting on an oscillating wing for the effects of compressibility. The calculations involved are generally quite tedious. Theodorsen and Garrick have suggested the simple correction $\sqrt[4]{1 - M^2}$ as a first approximation (reference 1). The results presented in figures 4 and 5 show that the experimental flutter speeds are lower in Freon-12 than in air at the same mass ratio (κ). This result represents, for the most part, a Mach number effect since the speed of sound in Freon-12 is about half of the speed of sound in air, and the Mach number is therefore higher in the former medium.

Inasmuch as model A had 15° sweepback, the Mach number component perpendicular to the leading edge ($M \cos \Lambda$) was used and the correction thus becomes $\sqrt[4]{1 - (M \cos \Lambda)^2}$. In figure 6 the compressibility correction for 0° and 15° sweep is plotted as a function of Mach number.

Figures 7 and 8 show the data corrected for compressibility. The adequacy of the correction is shown by the fact that the flutter speeds in the two mediums were superimposed throughout most of the density range.

Reduced-wave-length parameter.- Another factor which affects the air forces, and thereby the flutter velocity, results from the vibrating wing itself. The circulation, and therefore the lift of an oscillating airfoil is known to depend on the reduced-wave-length parameter $v/b\omega$. As $v/b\omega$ is increased, the air forces on the wing are increased and finally approach the steady-state value. Theodorsen has expressed this change in lift by means of the so-called F and G functions (reference 2). The total effect on the air forces is proportional to the absolute magnitude of the vector $\sqrt{F^2 + G^2}$. For a given density, these air forces are proportional to the velocity squared. The correction to be applied to the flutter speed is then $\sqrt[4]{F^2 + G^2}$. This factor is plotted as a function of the reduced-wave-length parameter in figure 9. An attempt is made in figures 10 and 11 to extract the effect of the reduced-wave-length parameter by multiplying the flutter speed by the factor $\sqrt[4]{F^2 + G^2}$.

Density.- Correcting the experimental flutter speeds for both Mach number and wave-length effects resulted in a straight-line plot, which

if extended, would pass through the origin. This result would seem to indicate that, in order to obtain simple bending-torsion flutter from a given model, a constant dynamic pressure is required. It should be pointed out, however, that this relationship may not be true for mass ratios and frequency ratios beyond the range encountered in this investigation.

Reynolds number.- If the experimental data are reduced to the form presented in figures 10 and 11, some insight may be gained as to the effects of Reynolds number. In figure 10 (model A), at any given density ratio, the data obtained in Freon-12 and those obtained in air have been nearly superimposed, even though the Reynolds numbers differed considerably. The Reynolds number is therefore concluded to have little or no effect upon the flutter speed of this model. Three flutter points of model B (fig. 11), however, fell considerably below the curve predicted by theory. These three points were made at test Reynolds numbers below 0.400×10^6. Inasmuch as the flutter speed is a function of the slope of the lift curve for the oscillating case, the Reynolds number might be expected to affect the flutter speed in the low Reynolds number range. The dash curve in figure 11 is the theoretical speed as determined by the two-dimensional potential-flow theory. These values are for incompressible speeds and have been multiplied by the function $\sqrt[4]{F^2 + G^2}$ in order to permit correlation with the experimental data. In the low-density range, for high values of $\sqrt{1/\kappa}$, the theoretical curve is noted to continue essentially as a straight line. The deviation of the experimental data from theory may therefore possibly be an effect of Reynolds number.

Tunnel-wall interference.- In order to interpret any abnormalities in the data that might arise from tunnel side-wall interference, two test sections of different configuration were employed. One section was 4.5 feet in diameter; whereas the other was the same section with side walls installed as shown in figure 1. Differences in flutter speed under corresponding conditions in the two test sections can be seen in figures 4 and 5. As these differences were of the same order of magnitude as the experimental error, the effects of changing the tunnel configuration were considered negligible.

CONCLUSIONS

An experimental investigation conducted of two uniform wings in the Langley flutter tunnel to determine the effects of density and Mach number on flutter speed indicated the following conclusions:

1. A simple compressibility correction was adequate to account for Mach number effects.

2. After the experimental data were corrected for compressibility and wave-length effects, the dynamic pressure at flutter was nearly constant over a wide range of densities.

3. No effects attributable to Reynolds number were found throughout most of the range tested. The results appear to indicate, however, that a Reynolds number effect may occur below a Reynolds number of 0.400×10^6.

4. A specific change in tunnel side-wall interference had no appreciable effect upon the flutter speed.

Langley Aeronautical Laboratory
National Advisory Committee for Aeronautics
Langley Air Force Base, Va., September 27, 1949

REFERENCES

1. Theodorsen, Theodore, and Garrick, I. E.: Mechanism of Flutter - A Theoretical and Experimental Investigation of the Flutter Problem. NACA Rep. 685, 1940.

2. Theodorsen, Theodore: General Theory of Aerodynamic Instability and the Mechanism of Flutter. NACA Rep. 496, 1935.

TABLE I.- EXPERIMENTAL DATA FOR MODEL A

Test	Test section dimension (ft)	Percentage of Freon-12	V_e (fps)	Mach number	ρ (slugs/cu ft)	Test Reynolds number	ω_e $\left(\frac{\text{rad}}{\text{sec}}\right)$	$\frac{V_e}{b\omega_e}$	$\frac{1}{\kappa}$	$\frac{V_e\sqrt[4]{F^2 + G^2}}{\sqrt[4]{1 - (M \cos \Lambda)^2}}$
1	4.5 diam.	0	379.5	0.335	0.00202	0.671×10^6	206.5	11.04	56.3	361.0
2	4.5 diam.	0	433.9	.384	.00150	.572	198.5	13.11	75.8	421.6
3	4.5 diam.	0	461.9	.409	.00128	.519	193.5	14.30	88.8	453.2
4	4.5 diam.	0	502.7	.444	.00103	.452	178.0	16.94	110.7	503.0
5	4.5 diam.	0	541.5	.481	.00080	.383	169.0	19.21	141.7	551.0
6	2 by 4.5	0	362.3	.326	.00227	.740	211.5	10.30	50.1	343.0
7	2 by 4.5	0	401.2	.353	.00171	.596	196.7	12.23	66.5	386.0
8	2 by 4.5	0	443.9	.390	.00136	.526	193.5	13.77	83.2	433.6
9	2 by 4.5	0	488.5	.432	.00109	.465	188.0	15.62	104.5	485.5
10	4.5 diam.	95.6	192.2	.382	.00829	2.022	207.0	5.57	13.7	174.7
11	4.5 diam.	95.5	216.1	.429	.00623	1.706	206.0	6.31	18.2	201.0
12	4.5 diam.	95.0	235.9	.467	.00503	1.506	207.0	6.83	22.5	223.0
13	4.5 diam.	94.0	258.2	.508	.00405	1.327	195.4	7.92	28.0	250.4
14	4.5 diam.	89.8	287.5	.567	.00321	1.202	193.5	8.92	35.4	288.0
15	4.5 diam.	90.0	311.0	.712	.00262	1.057	183.0	10.19	43.4	320.0
16	4.5 diam.	89.3	340.8	.668	.00200	.888	171.4	11.94	56.6	364.7
17	4.5 diam.	89.2	355.7	.696	.00171	.791	161.0	13.24	66.2	388.0
18	4.5 diam.	89.2	371.7	.726	.00144	.695	154.0	14.48	78.7	415.7
19	4.5 diam.	88.5	385.1	.752	.00126	.630	144.0	16.06	89.9	440.0
20	4.5 diam.	88.3	398.1	.773	.00113	.580	138.0	17.31	100.8	465.0
21	4.5 diam.	87.8	421.3	.818	.00088	.478	122.5	20.64	129.5	517.0
22	2 by 4.5	94.5	205.4	.409	.00757	1.999	211.0	5.84	15.0	188.7
23	2 by 4.5	90.0	245.0	.475	.00494	1.553	213.5	6.88	23.0	232.5
24	2 by 4.5	87.0	310.1	.602	.00276	1.109	191.0	9.74	41.1	317.0
25	2 by 4.5	85.9	348.3	.671	.00194	.877	177.0	11.81	58.5	373.0
26	2 by 4.5	82.0	378.5	.716	.00155	.768	169.0	13.45	73.2	418.5
27	2 by 4.5	83.7	412.7	.774	.00113	.609	145.0	17.09	100.0	482.0

TABLE II.- EXPERIMENTAL DATA FOR MODEL B

Test	Test section dimension (ft)	Percentage of Freon-12	V_e (fps)	Mach number	ρ (slugs/cu ft)	Test Reynolds number	ω_e $\left(\frac{rad}{sec}\right)$	$\frac{V_e}{b\omega_e}$	$\frac{1}{\kappa}$	$\frac{V_e\sqrt[4]{F^2+G^2}}{\sqrt[4]{1-(M\cos\Lambda)^2}}$
1	4.5 diam.	0	272.0	0.239	0.00206	0.975×10^6	196.7	4.15	37.9	235.0
2	4.5 diam.	0	301.5	.265	.00161	.845	196.0	4.62	48.5	264.0
3	4.5 diam.	0	328.8	.289	.00131	.751	193.5	5.10	59.5	292.5
4	4.5 diam.	0	356.2	.314	.00110	.679	192.5	5.54	71.6	321.0
5	4.5 diam.	0	394.3	.343	.00086	.595	191.6	6.17	90.6	362.1
6	4.5 diam.	0	419.7	.370	.00072	.530	189.7	6.63	108.1	388.0
7	4.5 diam.	0	464.7	.411	.00056	.459	188.5	7.40	138.6	437.0
8	4.5 diam.	0	491.6	.434	.00049	.419	187.2	7.88	160.6	470.0
9	4.5 diam.	0	511.7	.451	.00042	.364	185.3	8.28	187.2	492.0
10	4.5 diam.	0	530.8	.468	.00035	.328	184.1	8.65	221.0	515.0
11	4.5 diam.	0	513.7	.456	.00029	.266	184.1	8.37	266.5	495.0
12	2 by 4.5	0	255.3	.222	.00215	.934	193.5	3.96	36.3	219.0
13	2 by 4.5	0	293.4	.255	.00157	.787	-----	----	49.7	-----
14	2 by 4.5	0	318.3	.277	.00129	.702	190.4	5.01	60.5	279.0
15	2 by 4.5	0	353.5	.310	.00100	.612	187.9	5.64	78.1	318.0
16	2 by 4.5	0	374.1	.328	.00087	.564	188.5	5.95	89.8	339.5
17	2 by 4.5	0	403.4	.357	.00072	.510	87.2	6.46	108.5	371.0
18	2 by 4.5	0	421.0	.372	.00066	.490	87.9	6.72	118.0	389.5
19	4.5 diam.	96.0	142.3	.284	.00849	3.087	-----	----	9.2	-----
20	4.5 diam.	94.8	159.0	.316	.00658	2.662	-----	----	11.9	-----
21	4.5 diam.	93.1	175.3	.344	.00523	2.335	-----	----	14.0	-----
22	4.5 diam.	91.0	189.8	.370	.00424	2.051	-----	----	18.4	-----
23	4.5 diam.	89.2	210.1	.407	.00332	1.788	192.3	3.28	23.5	182.3
24	4.5 diam.	87.5	229.0	.442	.00272	1.598	189.1	3.63	28.8	202.7
25	4.5 diam.	87.2	237.5	.457	.00241	1.474	189.7	3.76	32.4	211.8
26	4.5 diam.	85.0	251.2	.481	.00213	1.384	187.2	4.02	36.6	227.0
27	4.5 diam.	84.2	266.3	.510	.00182	1.260	187.2	4.27	42.9	246.0
28	4.5 diam.	81.8	286.2	.542	.00151	1.126	183.5	4.68	51.8	269.0
29	4.5 diam.	78.8	308.2	.578	.00121	.975	182.8	5.06	64.6	297.0
30	4.5 diam.	75.8	340.3	.629	.00091	.812	180.9	5.64	86.0	339.0
31	2 by 4.5	88.2	148.2	.284	.00793	2.999	204.8	2.17	9.8	119.8
32	2 by 4.5	85.7	177.5	.336	.00509	2.296	200.4	2.66	15.3	148.2
33	2 by 4.5	84.5	214.2	.406	.00320	1.744	196.7	3.27	24.4	185.5
34	2 by 4.5	78.5	253.8	.468	.00207	1.342	191.0	3.99	37.9	228.5
35	2 by 4.5	77.6	291.9	.536	.00143	1.070	187.9	4.66	54.6	273.3
36	2 by 4.5	72.7	318.3	.576	.00112	.928	187.2	5.10	69.7	306.0
37	2 by 4.5	85.0	324.2	.633	.00107	.923	-----	----	73.0	-----
38	2 by 4.5	79.0	327.1	.621	.00106	.922	-----	----	73.7	-----
39	2 by 4.5	69.5	344.7	.613	.00088	.793	186.0	5.56	88.8	340.0

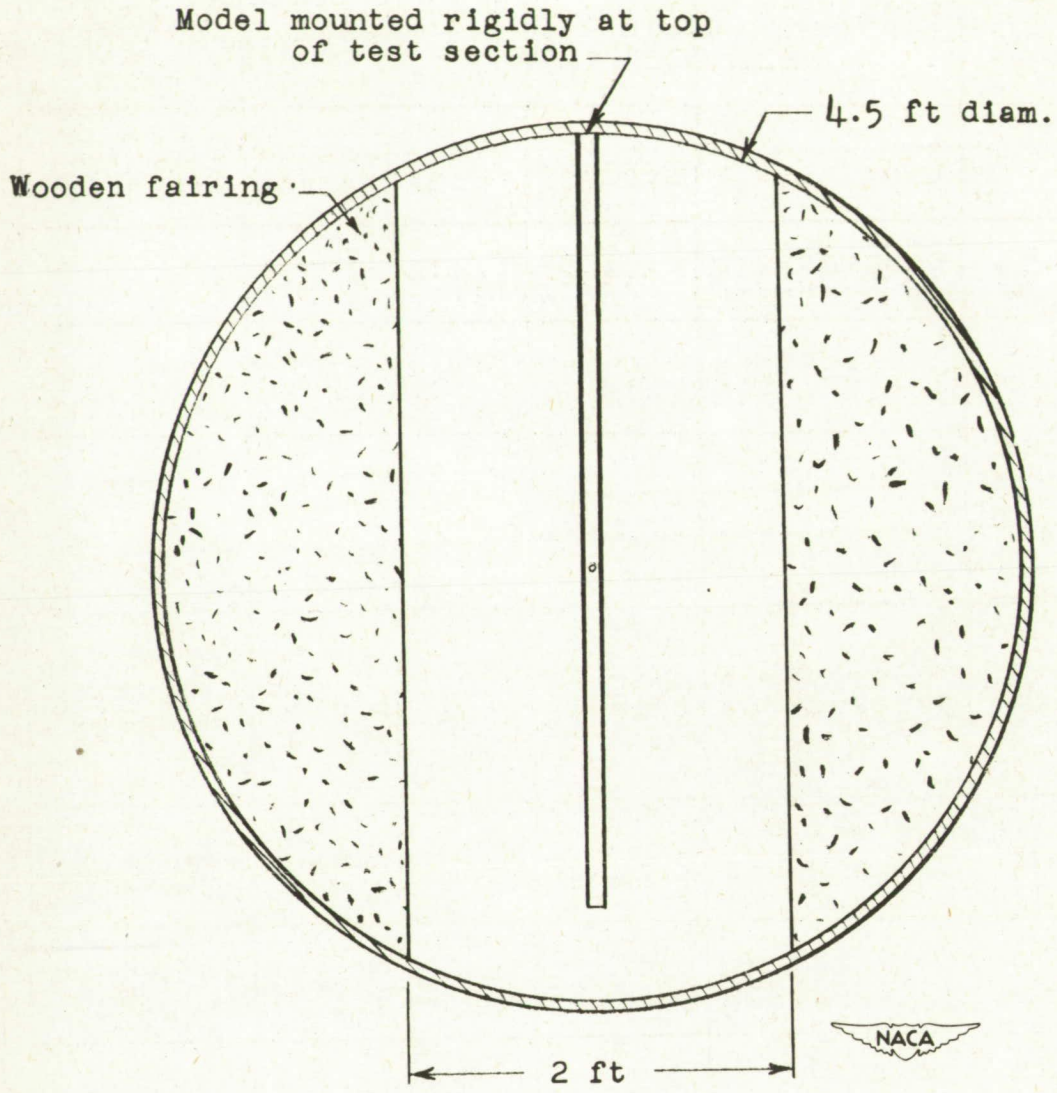

Figure 1.- Cross-sectional view of 2- by 4.5-foot test section.

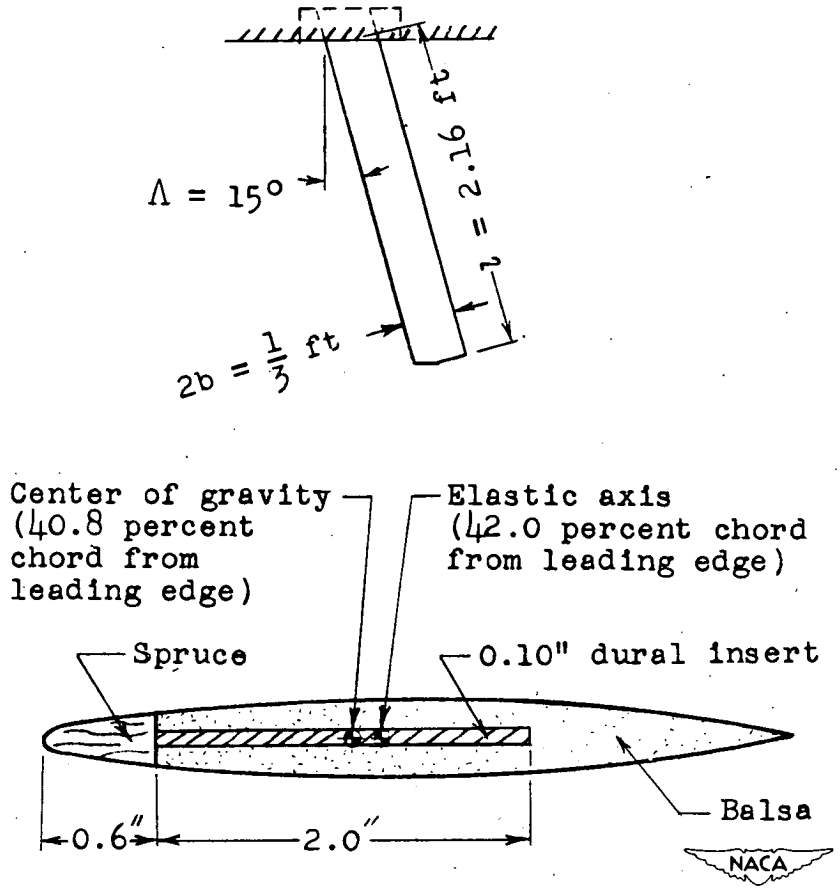

Figure 2.- Plan and cross-sectional views of model A.

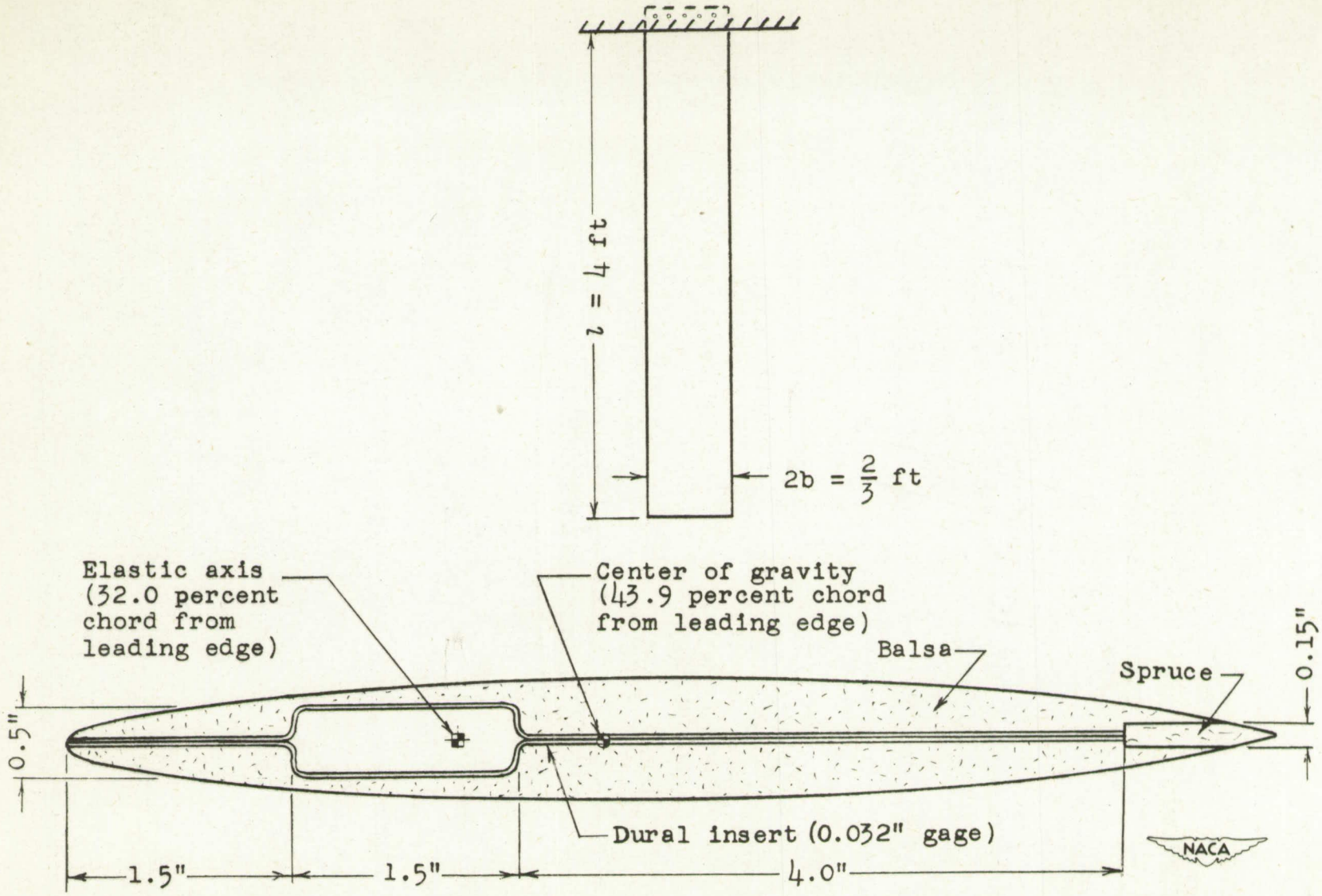

Figure 3.- Plan and cross-sectional views of model B.

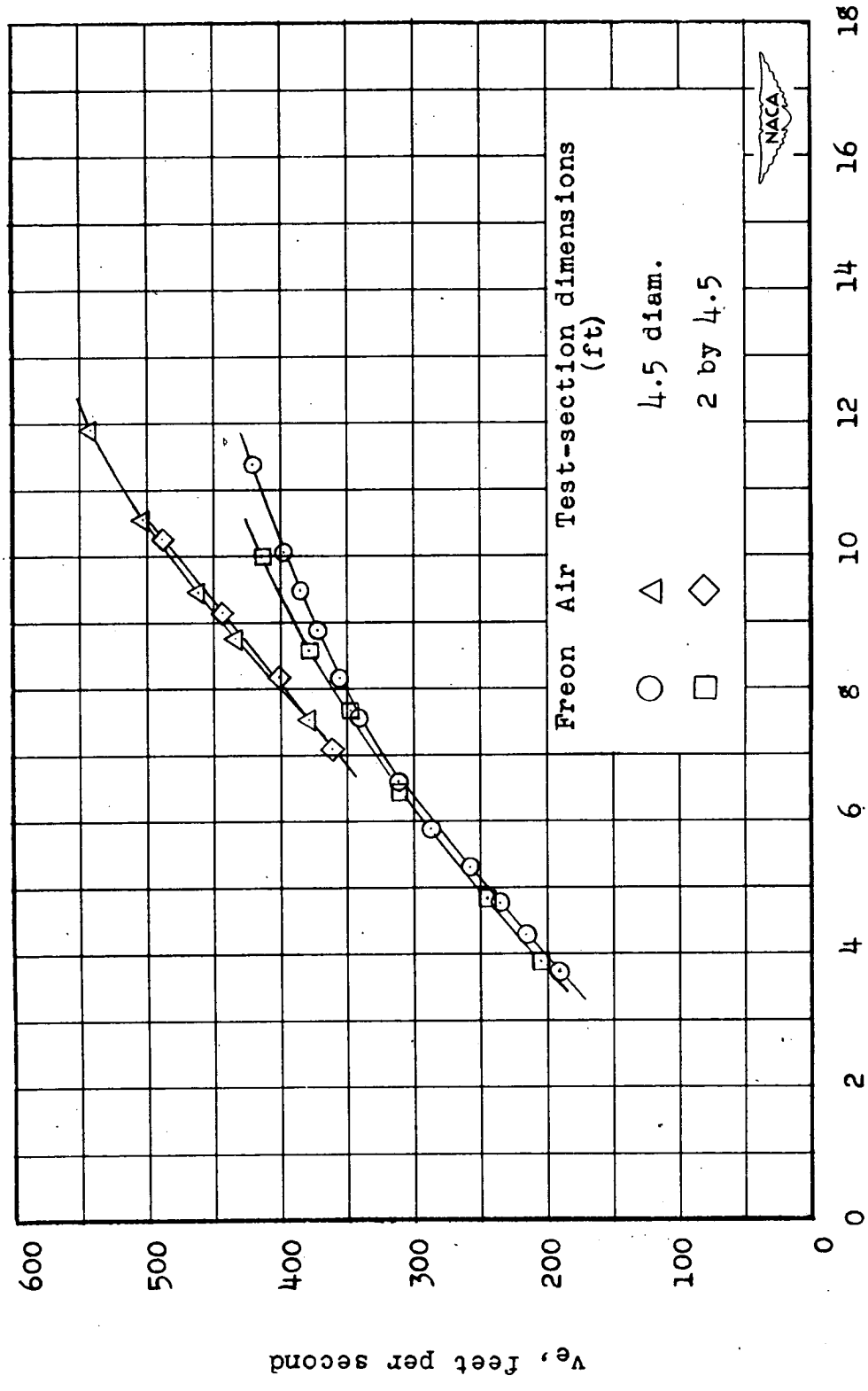

Figure 4.- Variation of experimental flutter speed with the square root of the mass ratio for model A.

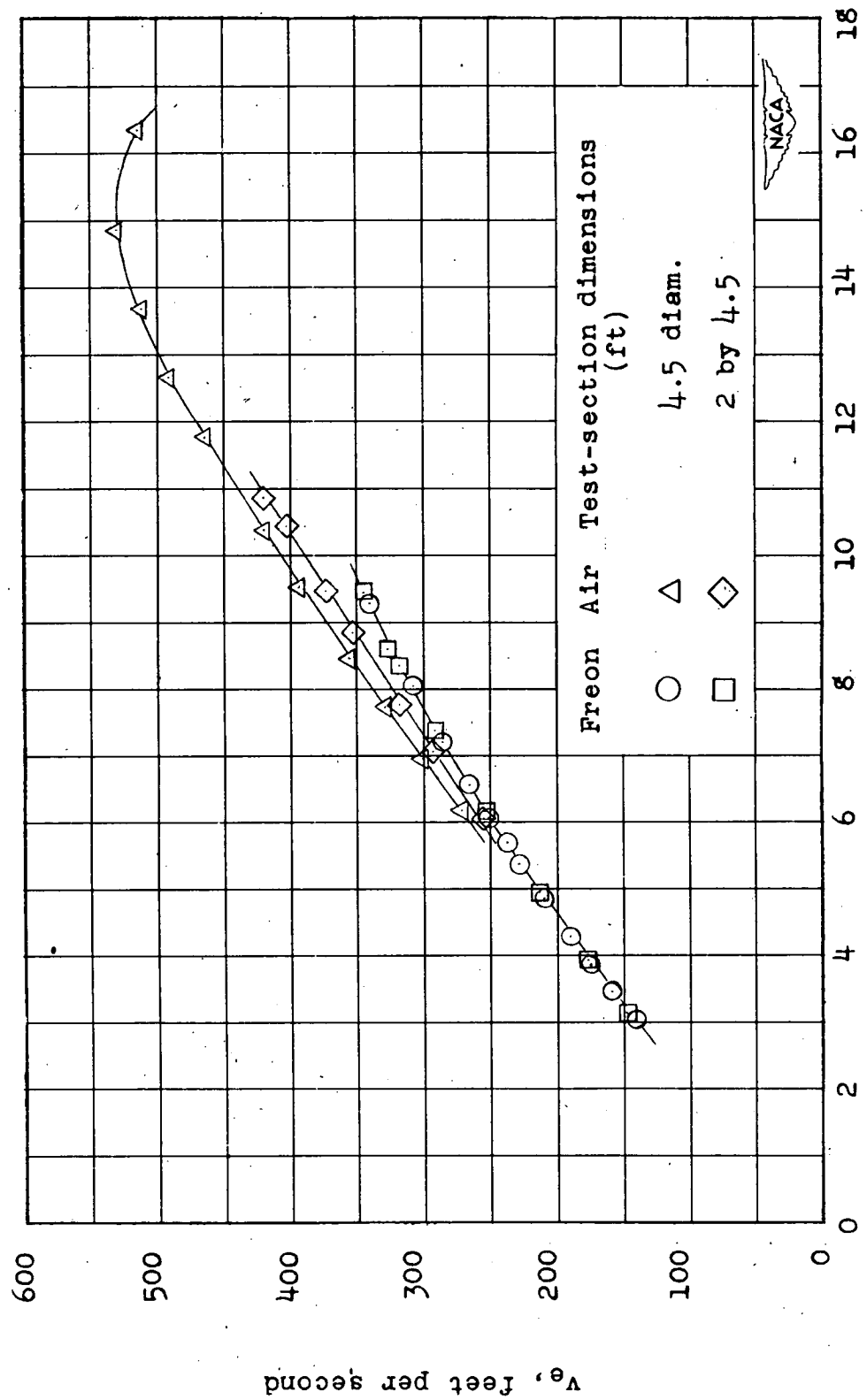

Figure 5.- Variation of experimental flutter speed with the square root of the mass ratio for model B.

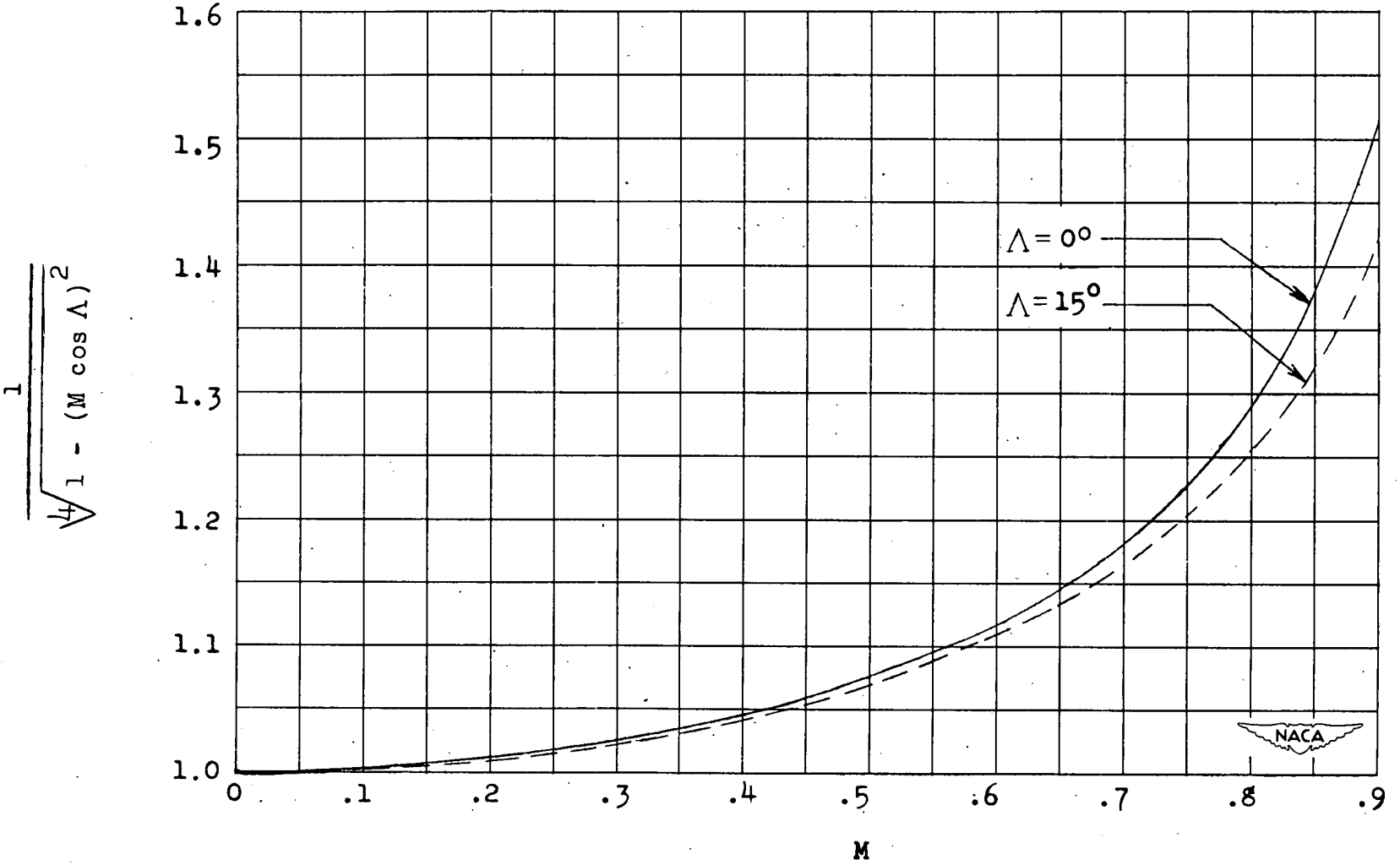

Figure 6.- Variation of $1/\sqrt[4]{1 - (M \cos \Lambda)^2}$ with Mach number.

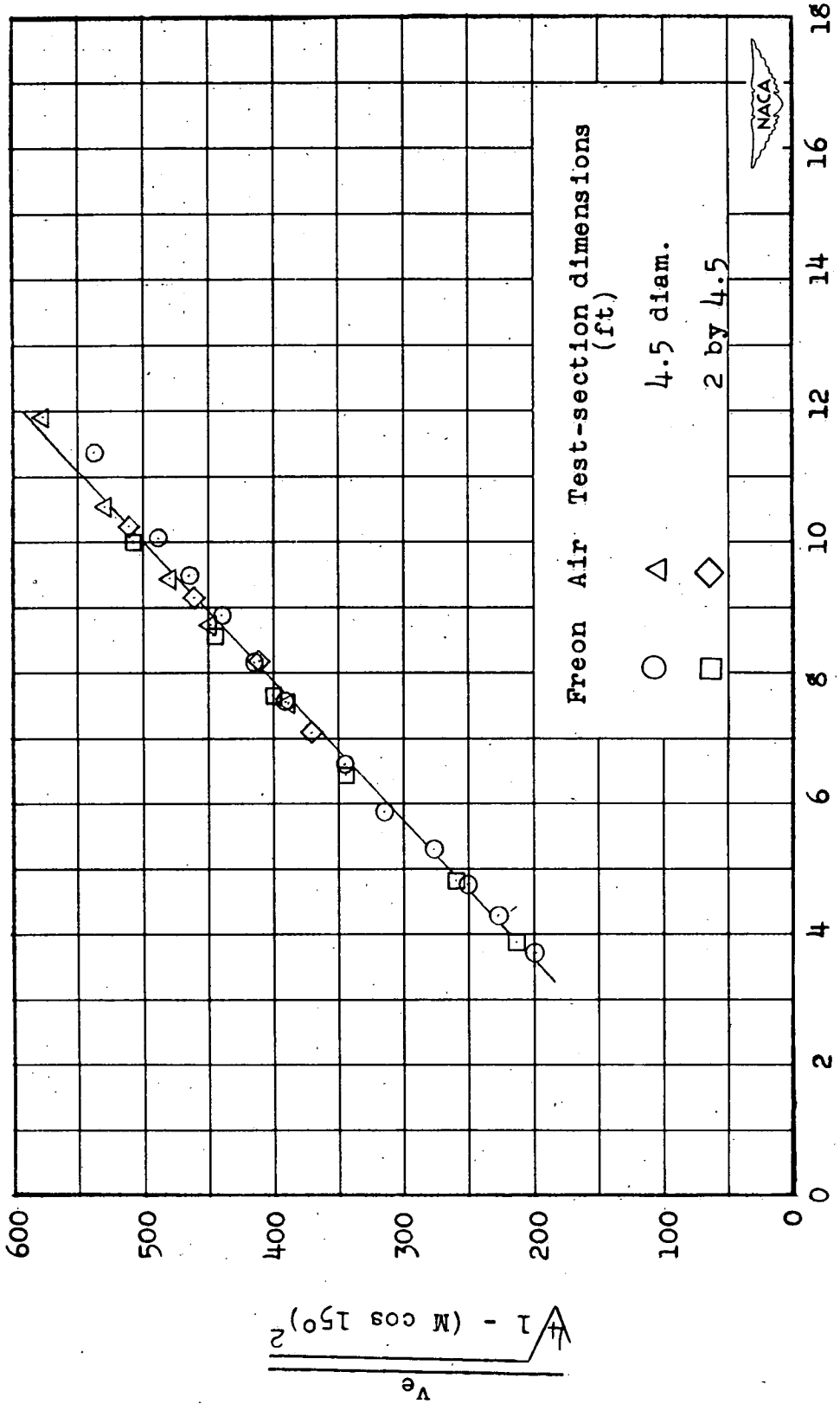

Figure 7.- Variation of incompressible flutter speed with the square root of the mass ratio for model A.

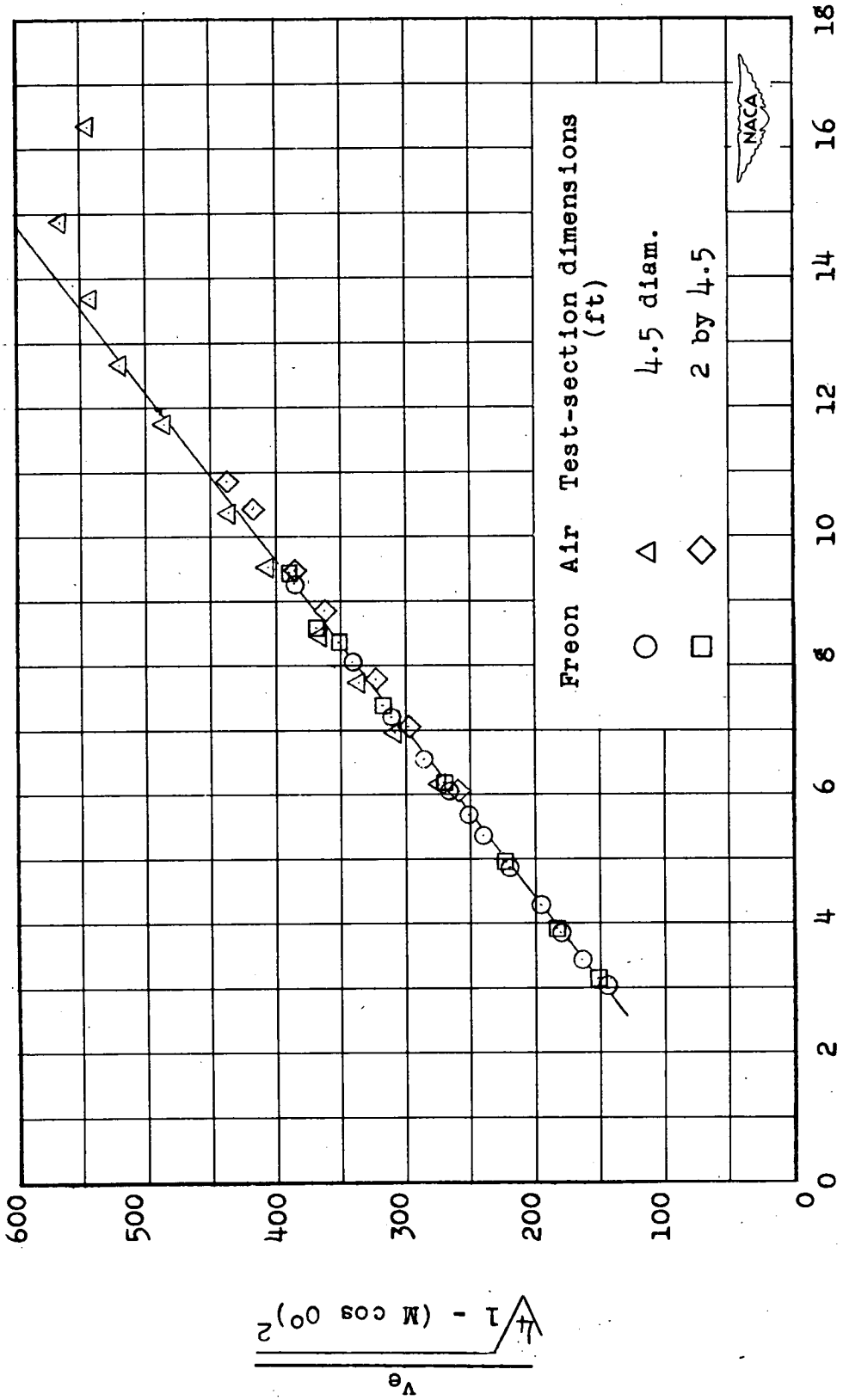

Figure 8.- Variation of incompressible flutter speed with the square root of the mass ratio for model B.

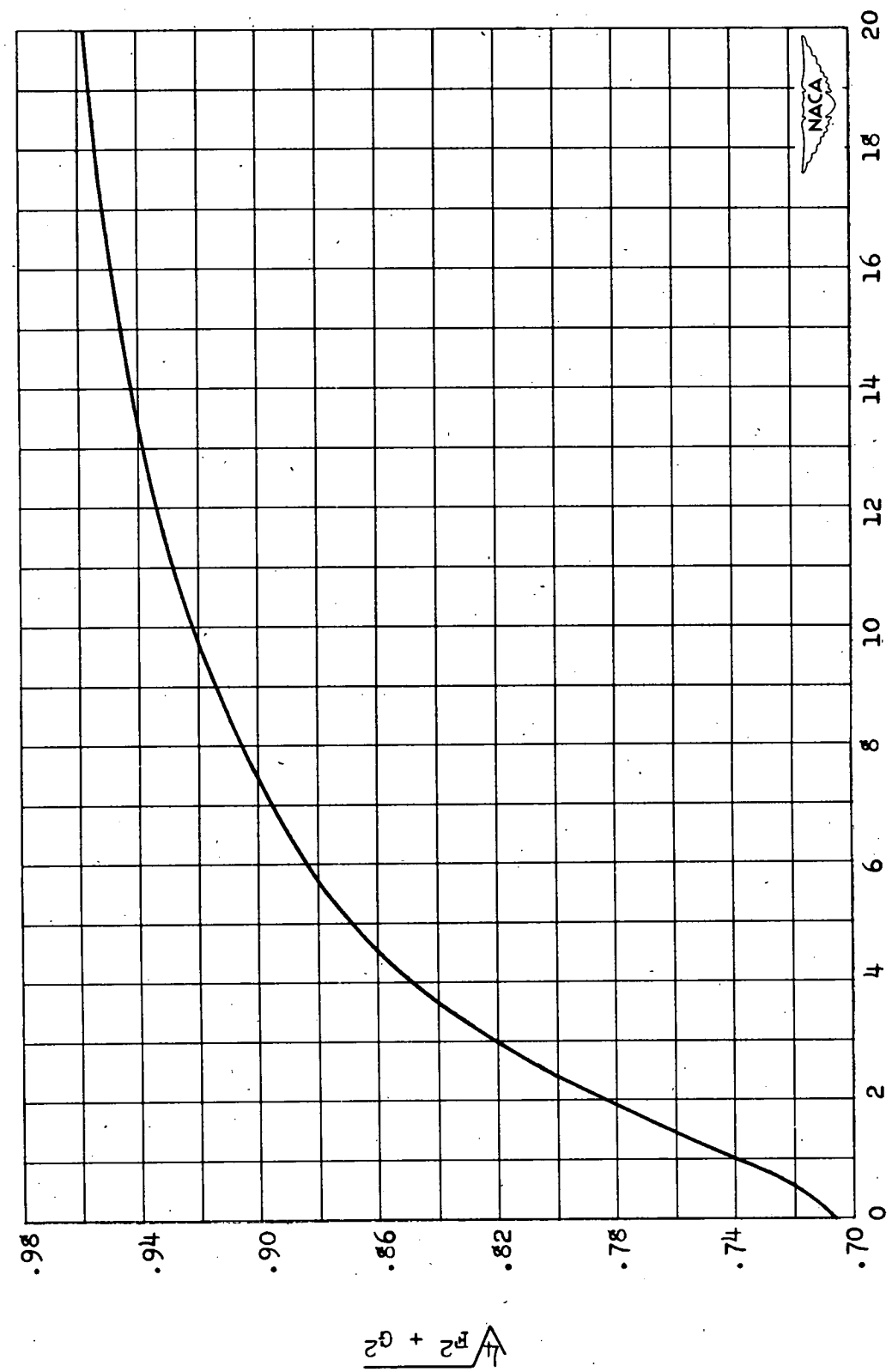

Figure 9.- Variation of $\sqrt[4]{F^2 + G^2}$ with reduced wave length.

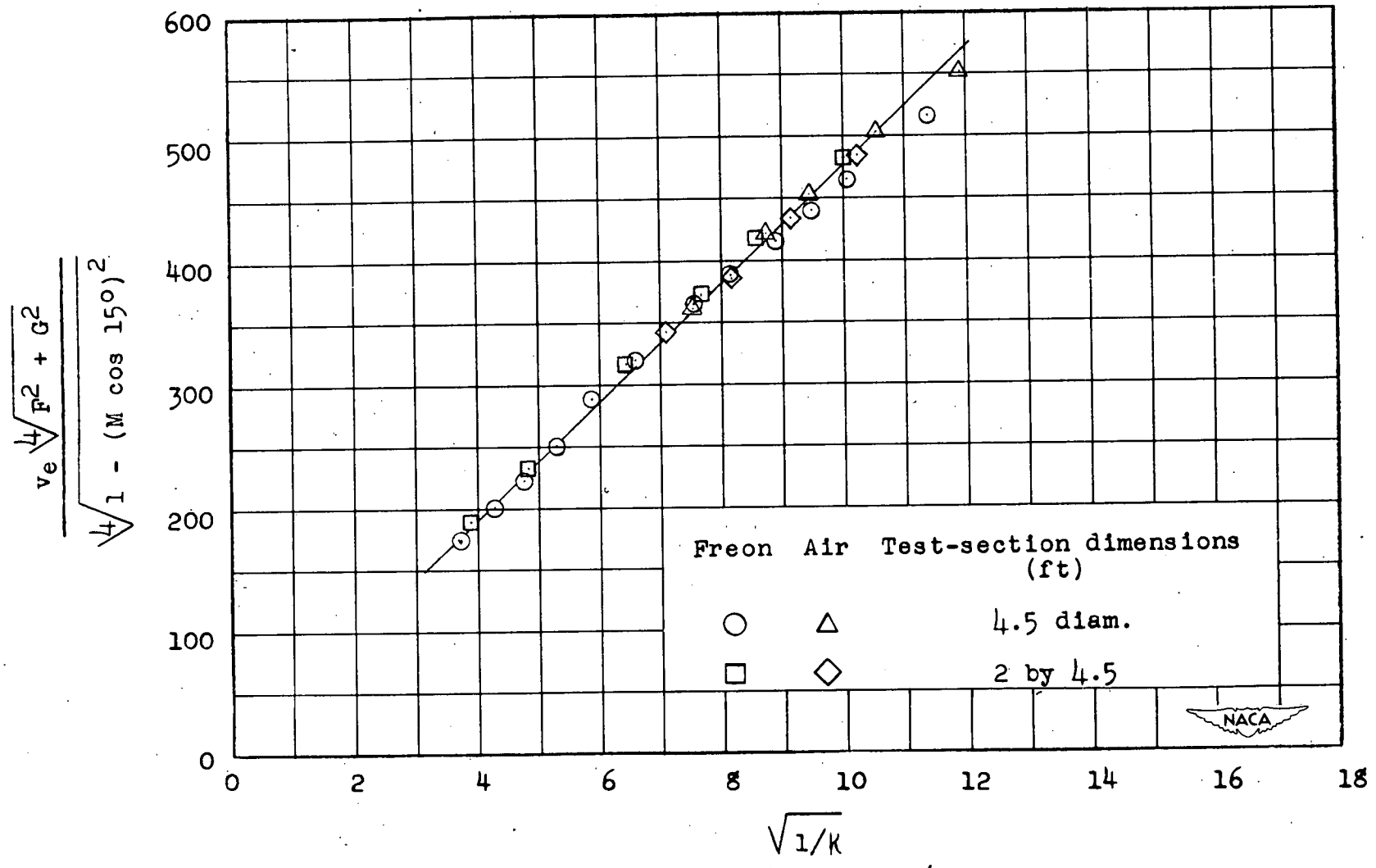

Figure 10.- Variation of $v_e \sqrt[4]{F^2 + G^2} \Big/ \sqrt[4]{1 - (M \cos \Lambda)^2}$ with the square root of the mass ratio for model A.

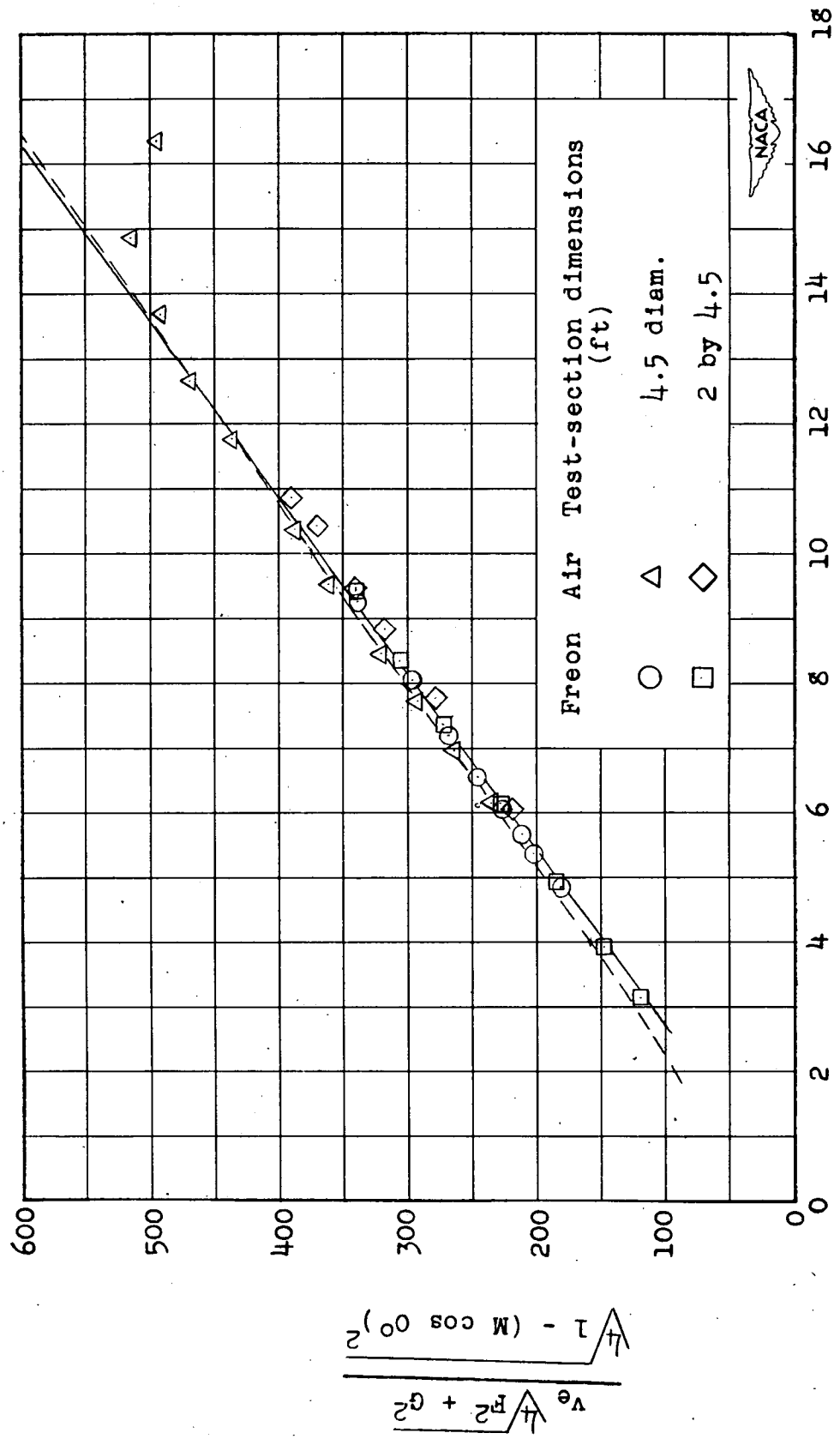

Figure 11.- Variation of $v_e \sqrt[4]{F^2 + G^2} \Big/ \sqrt[4]{1 - (M \cos \Lambda)^2}$ with $\sqrt{1/K}$ the square root of the mass ratio for model B.